Vietnam Journal of Mechanics, VAST, Vol. 43, No. 4 (2021), pp. 333 – 345
DOI: https://doi.org/10.15625/0866-7136/16272

REFLECTION AND TRANSMISSION OF P-WAVES AT A VERY ROUGH INTERFACE BETWEEN TWO ISOTROPIC ELASTIC SOLIDS

Pham Chi Vinh[1,*], Do Xuan Tung[2], Nguyen Thi Kieu[2]
[1]*Faculty of Mathematics, Mechanics and Informatics, VNU Hanoi University of Science, 334 Nguyen Trai street, Thanh Xuan district, Hanoi, Vietnam*
[2]*Faculty of Civil Engineering, Hanoi Architectural University, Km 10 Nguyen Trai street, Thanh Xuan district, Hanoi, Vietnam*
[*]E-mail: pcvinh@vnu.edu.vn

Received: 12 June 2021 / Published online: 04 November 2021

Abstract. This paper deals with the reflection and transmission of P-waves at a very rough interface between two isotropic elastic solids. The interface is assumed to oscillate between two straight lines. By mean of homogenization, this problem is reduced to the reflection and transmission of P-waves through an inhomogeneous orthotropic elastic layer. It is shown that a P incident wave always creates two reflected waves (one P wave and one SV wave), however, there may exist two, one or no transmitted waves. Expressions in closed-form of the reflection and transmission coefficient have been derived using the transfer matrix of an orthotropic elastic layer. Some numerical examples are carried out to examine the reflection and transmission of P-waves at a very rough interface of tooth-comb type, tooth-saw type and sin type. It is found numerically that the reflection and transmission coefficients depend strongly on the incident angle, the incident wave frequency, the roughness and the type of interfaces.

Keywords: reflection, transmission, very rough interfaces, P waves, SV waves.

1. INTRODUCTION

The reflection and transmission of waves at rough boundaries and interfaces have given much attention to researchers due to their important applications in Seismology and Geophysics, because the Earth's surface and the interfaces between different layers of the Earth crust are really rough, not flat. Most of the studies considered slightly rough boundaries and interfaces, see for examples, works [1, 2], and the perturbation method [3] was employed to analyze the problems. However, due to the mathematical complexity caused by strong roughness of boundaries and interfaces, there are few studies concerning the reflection and transmission of waves at very rough boundaries and interfaces [4, 5]. The traditional formulation of this problem leads to boundary integral equations whose numerical solution is unstable due to rapid oscillation of rough boundaries and interfaces. To overcome this obstacle, the composite material layer containing very rough interface is replaced by a homogenized material layer by mean of homogenization [6]. Then, the problem is reduced to the reflection and transmission of waves through the homogenized material layer. To solve this problem we need homogenized equations governing motion of the homogenized material layer. The explicit homogenized equations for one-component waves such as SH (shear horizontal) waves, TE (transverse electric) waves and TM (transverse magnetic) waves were first found [7,8]. However, those for more than one-component waves were found only recently [9, 10].

In this paper, we consider the reflection and transmission of P-waves, two-component wave, at a very rough interface between two isotropic elastic solids that oscillates between two straight lines. By mean of homogenization, this problem is reduced to the reflection and transmission of P-waves through an inhomogeneous orthotropic elastic layer whose motion is governed by the homogenized equations of the elasticity theory [9, 11]. It is shown that there always exist two reflected waves (one P wave and one SV wave) for a given P incident wave, however, there may exist two, one or no transmitted waves. Formulas in closed-form of the reflection and transmission coefficient have been obtained using the transfer matrix method. These formulas can be used as convenient tool to determine the internal characteristics of the Earth crust from the signals of reflected and transmitted waves. They may be helpful in exploration of the valuable materials such as minerals, crystals and metals etc. Some numerical examples are carried out to examine the reflection and transmission of P-waves at very rough interfaces of tooth-comb type, tooth-saw type and sin type. It is found numerically that the reflection and transmission coefficients depend strongly on the incident angle, the incident wave frequency, the roughness and the type of interfaces.

2. STATEMENT OF THE PROBLEM

Consider a unbounded linear isotropic elastic body occupied two-dimensional domains Ω^+ and Ω^- of the plane x_1x_2 whose interface is the curve L expressed by equation: $x_2 = h(x_1/\epsilon)$=$h(y)$, where $h(y)$ is a periodic function of period 1 whose minimum and

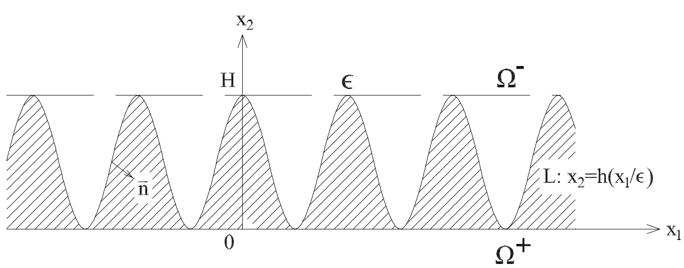

Fig. 1. Two-dimensional domains Ω^+ and Ω^- have a very rough interface L expressed by equation $x_2 = h(x_1/\epsilon)$=$h(y)$, where $h(y)$ is a periodic function with period 1. The curve L highly oscillates between the parallel straight lines $x_2 = 0$ and $x_2 = H$

maximum values being 0 and H, respectively (see Fig. 1), ϵ assumed to be much more small than H (i. e. the curve L is a very rough interface). The interface L lies in the strip $0 < x_2 < H$. We also assume that, in the domain $0 < x_1 < \epsilon$, i.e. $0 < y < 1$, any straight line $x_2 = x_2^0 = \text{const}$ $(0 < x_2^0 < H)$ has exactly two intersections with the curve L. That means, in the interval $0 < y < 1$ the equation $h(y) = x_2$ for y has exactly two roots denoted by $y_1(x_2)$ and $y_1(x_2)$ $(0 < y_1(x_2) < y_2(x_2) < 1)$. Suppose the elastic half-spaces Ω^+ and Ω^- are characterized respectively by the Lame constants μ^+, λ^+ and μ^-, λ^-, the mass densities ρ^+ and ρ^-. That means, the Lame constants and the mass density of the elastic body are defined as

$$\mu, \lambda, \rho = \begin{cases} \mu^+, \lambda^+, \rho^+ & \text{for } x_2 < h(x_1/\epsilon) \\ \mu^-, \lambda^-, \rho^- & \text{for } x_2 > h(x_1/\epsilon) \end{cases} \tag{1}$$

where $\mu^+, \mu^-, \lambda^+, \lambda^-, \rho^+, \rho^-$ are constant. We are interested in the propagation of P-waves whose displacements are of the form

$$u_k = u_k(x_1, x_2, t)\ (k = 1, 2),\ u_3 \equiv 0. \tag{2}$$

In the absence of the body forces, the equations governing the motion of P-waves are

$$\sigma_{11,1} + \sigma_{12,2} = \rho \ddot{u}_1,\ \sigma_{12,1} + \sigma_{22,2} = \rho \ddot{u}_2, \tag{3}$$

where σ_{ij} are stress components, commas signify differentiation with respect to x_k, a dot indicates differentiation with respect to the time t. For isotropic elastic materials, the strain-stress relation is of the form

$$\sigma_{11} = (\lambda + 2\mu)u_{1,1} + \lambda u_{2,2},\ \sigma_{22} = (\lambda + 2\mu)u_{2,2} + \lambda u_{1,1},\ \sigma_{12} = \mu(u_{1,2} + u_{2,1}). \tag{4}$$

Suppose Ω^+ and Ω^- are welded with each other along the interface L. Then, the displacement and stresses are required to be continuous through the curve L. In particular, we have

$$[u_k]_L = 0,\ \Big[\sigma_{k1}n_1 + \sigma_{k2}n_2\Big]_L = 0\ (k = 1, 2), \tag{5}$$

where $[\varphi]_L$ signifies the jump of φ through the interface L, $\mathbf{n} = (n_1, n_2, 0)$ is the unit normal to L (see Fig. 1).

Let an incident P-wave with the unit displacement amplitude, the incident angle θ_0, the wave number k_0 and the phase velocity v_0, to propagate in the half-space Ω^+. Then, its displacements u_{1I}, u_{2I} are given by [12]

$$u_1^0 = \sin\theta_0 e^{ik_0(x_1 sin\theta_0 + x_2 cos\theta_0 - v_0 t)},\ u_2^0 = \cos\theta_0 e^{ik_0(x_1 sin\theta_0 + x_2 cos\theta_0 - v_0 t)}, \tag{6}$$

where $v_0 = \sqrt{(\lambda^+ + 2\mu^+)/\rho^+}$. Note that $k_0 v_0 = \omega$ where ω is the circular wave frequency.

We are interested in the reflection and transmission of the P-wave given by (6) at the very rough interface L.

3. REFLECTION AND TRANSMISSION OF P-WAVES BY MEANS OF HOMOGENIZATION

By means of homogenization, the reflection and transmission of the incident P-wave given by (6) at the very rough interface L is reduced to its reflection and transmission through an elastic layer occupying the domain $0 < x_2 < H$ that is sandwiched between two isotropic elastic half-spaces Ω^+ $(x_2 < 0)$ and Ω^- $(x_2 > H)$ (see Fig. 2). The layer's motion is governed by the explicit homogenized equations derived by Vinh and Tung [9, 11]. In particular, the equations of motion are

$$\bar{\sigma}_{11,1} + \bar{\sigma}_{12,2} = \bar{\rho}\ddot{\bar{u}}_1, \ \bar{\sigma}_{12,1} + \bar{\sigma}_{22,2} = \bar{\rho}\ddot{\bar{u}}_2, \tag{7}$$

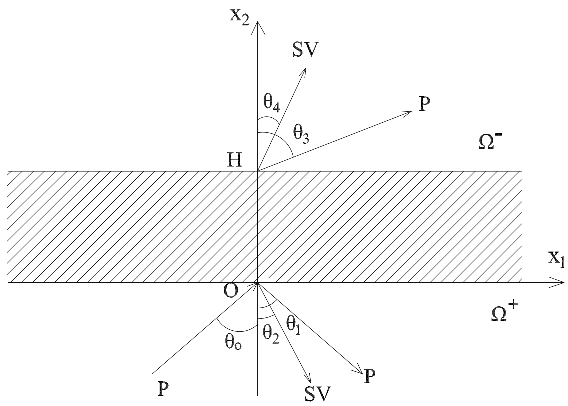

Fig. 2. The reflection and transmission of a P-wave at a very rough interface by means of homogenization

and the stress-strain relation takes the form

$$\bar{\sigma}_{11} = \bar{c}_{11}\bar{u}_{1,1} + \bar{c}_{12}\bar{u}_{2,2}, \ \bar{\sigma}_{22} = \bar{c}_{12}\bar{u}_{1,1} + \bar{c}_{22}\bar{u}_{2,2}, \ \bar{\sigma}_{12} = \bar{c}_{66}(\bar{u}_{1,2} + \bar{u}_{2,1}), \tag{8}$$

where

$$\begin{aligned} &\bar{c}_{11} = \langle(\lambda+2\mu)^{-1}\rangle^{-1}, \bar{c}_{12} = \langle(\lambda+2\mu)^{-1}\rangle^{-1}\langle\lambda(\lambda+2\mu)^{-1}\rangle, \ \bar{c}_{66} = \langle\mu^{-1}\rangle^{-1} \\ &\bar{c}_{22} = \Big(\langle(\lambda+2\mu)\rangle + \langle(\lambda+2\mu)^{-1}\rangle^{-1}\langle\lambda(\lambda+2\mu)^{-1}\rangle^2 - \langle\lambda^2(\lambda+2\mu)^{-1}\rangle\Big), \ \bar{\rho} = \langle\rho\rangle. \end{aligned} \tag{9}$$

Here we use the notation

$$\langle f \rangle := \big[y_2(x_2) - y_1(x_2)\big]f^- + \big[1 - y_2(x_2) + y_1(x_2)\big]f^+, \tag{10}$$

with f^+ and f^- are (constant) values of f corresponding to the half-space Ω^+ and Ω^-, respectively. According to (8) and (9), (10), the elastic layer $0 < x_2 < H$ is orthotropic and inhomogeneous, in general, and its elastic constants $\bar{c}_{ij}$ depend on x_2. However, when the interface L is of the tooth-comb type, as shown in Fig. 3, the elastic layer becomes homogeneous and its elastic constants $\bar{c}_{ij}$ are computed by (9) in which the average value of quantities is calculated by

$$\langle f \rangle := \frac{1}{a+b}(af^+ + bf^-) \tag{11}$$

The motion of isotropic elastic half-spaces Ω^+ $(x_2 < 0)$ and Ω^- $(x_2 > H)$ is governed by Eqs. (3) and (4). In addition, is required the continuity of displacements and stresses at the interfaces $x_2 = 0$ and $x_2 = H$.

3.1. Tooth-comb-type interfaces

In this section, we consider the reflection and transmission of P-wave at a very rough interface that is of tooth-comb type (Fig. 3). The material layer $0 < x_2 < H$ is a homogeneous orthotropic elastic layer whose elastic constants $\bar{c}_{ij}$ are computed by (9) and (11), as mentioned above.

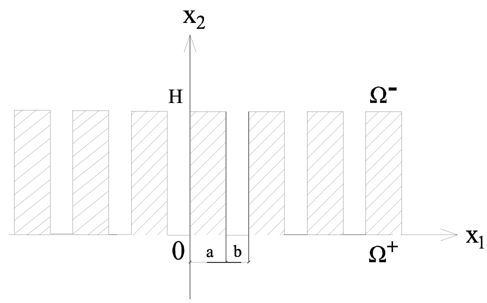

Fig. 3. Tooth-comb type interface

3.1.1. *Incident wave and reflected, transmitted waves*

a. Incident wave

As stated in Section 2, the incident wave is a P wave propagating in the half-space Ω^+ with the displacements given by (6). From (6) we have

$$u_1^0 = U_1^0(y)\, e^{ik(x_1-ct)},\ u_2^0 = U_2^0(y)\, e^{ik(x_1-ct)},\ y = kx_2, \tag{12}$$

where

$$U_1^0(y) = \sin\theta_0\, e^{i\, y\cot\theta_0},\ U_2^0(y) = \cos\theta_0\, e^{i\, y\cot\theta_0}, \tag{13}$$

and $k = k_0\, \sin\theta_0$, $c = v_0/\sin\theta_0$. From (4), (12) and (13) it follows

$$\sigma_{12}^0 = kT_1^0(y)e^{ik(x_1-ct)},\ \sigma_{22}^0 = kT_2^0(y)e^{ik(x_1-ct)}, \tag{14}$$

where

$$\begin{aligned} T_1^0(y) &= 2i\mu^+ \cos\theta_0 e^{iy\cot\theta_0}, \\ T_2^0(y) &= i[\lambda^+ \sin\theta_0 + (\lambda^+ + 2\mu^+)\cos^2\theta_0/\sin\theta_0]e^{i\, y\cot\theta_0}. \end{aligned} \tag{15}$$

Let $\boldsymbol{\xi}^0(y) = [U_1^0(y)\ \ U_2^0(y)\ \ T_1^0(y)\ \ T_2^0(y)]^T$. Then, we have

$$\boldsymbol{\xi}^0(y) = \boldsymbol{\xi}_I^0\, e^{i\, y\cot\theta_0},\ \boldsymbol{\xi}_I^0 = \begin{bmatrix} \sin\theta_0 \\ \cos\theta_0 \\ 2i\mu^+\cos\theta_0 \\ i[\lambda^+\sin\theta_0 + (\lambda^+ + 2\mu^+)\cos^2\theta_0/\sin\theta_0] \end{bmatrix}. \tag{16}$$

When impinging on the interface $x_2 = 0$, the P incident wave (6) creates reflected waves propagating in the half-space Ω^+, transmitted waves traveling in the half-space Ω^- and reflected-transmitted waves propagating in the layer.

b. Reflected waves

It is well-known that the slowness section C of compressible isotropic materials in the (s_1, s_2)-plane contains two separate circles with radii $s_L = 1/c_L$ and $s_T = 1/c_T$ [12], where $c_L = \sqrt{(\lambda+2\mu)/\rho}$, $c_T = \sqrt{(\mu)/\rho}$ $(0 < s_L < s_T)$, as shown in Fig. 4 for the half-space Ω^+ and Fig. 5 for the half-space Ω^-. In addition, the s_1-component of the slowness vectors of reflected waves, say s_1^r, and of transmitted waves, say s_1^t, are equal to each other and equal to the one of the incident wave (6), namely: $s_1^0 = s_L^+ \sin\theta_0$, according to Snell's law, i. e.

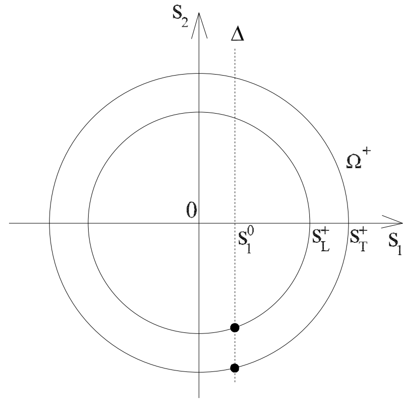

Fig. 4. Slowness section of Ω^+

$$s_1^r = s_1^t = s_1^0 = s_L^+ \sin\theta_0. \tag{17}$$

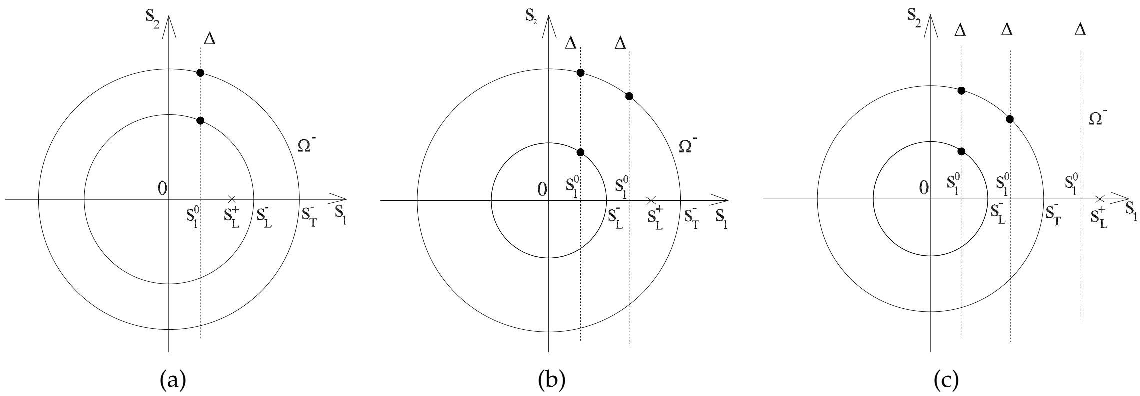

Fig. 5. Slowness section of Ω^- for three cases

By Δ we denote the straight line $s_1 = s_1^0\,(= s_1^r = s_1^t)$ for a given $\theta_0 \in (0, \pi/2)$. From Fig. 4 and the fact: $0 < s_1^0 < s_L^+ \;\forall\,\theta_0 \in (0, \pi/2)$, one can see that the straight line Δ always has four different intersections with the slowness section C^+ of the half-space Ω^+. That means: for any incident angle $\theta_0 \in (0, \pi/2)$, the P incident wave (6) establishes exactly two reflected waves, one P wave with the reflection angle $\theta_1 = \theta_0$ and one SV wave with the reflection angle $\theta_2 = \arcsin(c_T^+ \sin\theta_0 / c_L^+)$ $(0 < \theta_2 < \theta_1)$ (see Fig. 2). Note that

$$s_L^+ \sin\theta_1 = s_T^+ \sin\theta_2 = s_1^r = s_1^0 = s_L^+ \sin\theta_0. \tag{18}$$

Let u_n^1 and σ_{n2}^1 $(n = 1, 2)$ be the displacements and stresses of the P reflected wave and u_n^2 and σ_{n2}^2 $(n = 1, 2)$ be those of the SV reflected wave. It is clear that

$$u_n^m = U_n^m(y)\, e^{ik(x_1 - ct)},\;\; \sigma_{n2}^m = kT_n^m(y)\, e^{ik(x_1 - ct)},\;\; n, m = 1, 2 \tag{19}$$

where the amplitude vectors $\boldsymbol{\xi}^m(y) = [U_1^m(y)\ U_2^m(y)\ T_1^m(y)\ T_2^m(y)]^T\,(m = 1,2)$ are given by

$$\boldsymbol{\xi}^1(y) = A_1\boldsymbol{\xi}_r^1\, e^{-i\,y\cot\theta_0},\ \boldsymbol{\xi}_r^1 = \begin{bmatrix} \sin\theta_0 \\ -\cos\theta_0 \\ -2i\mu^+\cos\theta_0 \\ i\left[\lambda^+\sin\theta_0 + (\lambda^+ + 2\mu^+)\cos^2\theta_0/\sin\theta_0\right] \end{bmatrix}, \tag{20}$$

and

$$\boldsymbol{\xi}^2(y) = A_2\boldsymbol{\xi}_r^2\, e^{-i\,y\cot\theta_2},\ \boldsymbol{\xi}_r^2 = \begin{bmatrix} \cos\theta_2 \\ \sin\theta_2 \\ i\mu^+(\sin\theta_2 - \cos^2\theta_2/\sin\theta_2) \\ -2i\mu^+\cos\theta_2 \end{bmatrix}, \tag{21}$$

$A_k\,(k = 1,2)$ are constants to be determined and $|A_k|\,(k = 1,2)$ are called the reflection coefficients.

c. Transmitted waves

- *Case 1:* $0 < s_L^+ \le s_L^-$

From Fig. 5(a) and the fact: $s_1^0 < s_L^+ \le s_L^-$, it follows that for this case the P incident wave (6) creates two transmitted waves, one P wave with the transmission angle θ_3 and one SV wave with the transmission angle θ_4, for any $\theta_0 \in (0, \pi/2)$, see Fig. 2. The transmission angles are computed using Snell's law (17). In particular, we have: $\theta_3 = \arcsin(s_L^+\sin\theta_0/s_L^-)$ and $\theta_4 = \arcsin(s_L^+\sin\theta_0/s_T^-)$ $(0 < \theta_4 < \theta_3)$. Note that

$$s_L^-\sin\theta_3 = s_T^-\sin\theta_4 = s_1^t = s_1^0 = s_L^+\sin\theta_0. \tag{22}$$

Let u_n^3 and $\sigma_{n2}^3\,(n = 1,2)$ be the displacements and stresses of the P transmitted wave and u_n^4 and $\sigma_{n2}^4\,(n = 1,2)$ be those of the SV transmitted wave. One can see that

$$u_n^m = U_n^m(y)\,e^{ik(x_1 - ct)},\ \sigma_{n2}^m = kT_n^m(y)\,e^{ik(x_1 - ct)},\ n = 1,2,\ m = 3,4 \tag{23}$$

where the amplitude vectors $\boldsymbol{\xi}^m(y) = [U_1^m(y)\ U_2^m(y)\ T_1^m(y)\ T_2^m(y)]^T\,(m = 3,4)$ are calculated by

$$\boldsymbol{\xi}^3(y) = A_3\boldsymbol{\xi}_t^3\, e^{i\,y\cot\theta_3},\ \boldsymbol{\xi}_t^3 = \begin{bmatrix} \sin\theta_3 \\ \cos\theta_3 \\ 2i\mu^-\cos\theta_3 \\ i[\lambda^-\sin\theta_3 + (\lambda + 2\mu)^-\cos^2\theta_3/\sin\theta_3] \end{bmatrix}, \tag{24}$$

and

$$\boldsymbol{\xi}^4(y) = A_4\boldsymbol{\xi}_t^4\, e^{i\,y\cot\theta_4},\ \boldsymbol{\xi}_t^4 = \begin{bmatrix} -\cos\theta_4 \\ \sin\theta_4 \\ i\mu^-(\sin\theta_4 - \cos^2\theta_4/\sin\theta_4) \\ 2i\mu^-\cos\theta_4 \end{bmatrix}, \tag{25}$$

$A_k\,(k = 3,4)$ are constants to be determined and $|A_k|\,(k = 3,4)$ are called the transmission coefficients.

- *Case 2:* $s_L^- < s_L^+ \le s_T^-$

It follows from Fig. 5(b):

(i) For $0 < s_1^0 \le s_L^- \Leftrightarrow 0 < \theta_0 \le \theta_0^1 = \arcsin(s_L^-/s_L^+)$, there exist two transmitted waves, one P wave and one SV wave.

(ii) For $s_L^- < s_0^1 < s_L^+ \Leftrightarrow \theta_0 \in (\theta_0^1, \pi/2)$; there exist only SV transmitted wave. The P transmitted wave becomes a surface wave.

- *Case 3:* $s_L^+ > s_T^-$

Fig. 5(c) indicates three possibilities:

(i) For $0 < s_1^0 \le s_L^- \Leftrightarrow 0 < \theta_0 \le \theta_0^1 = \arcsin(s_L^-/s_L^+)$, there exist two transmitted waves, one P wave and one SV wave.

(ii) For $s_L^- < s_0^1 \le s_T^- \Leftrightarrow \theta_0^1 < \theta_0 \le \theta_0^2 = \arcsin(s_T^-/s_L^+)$; there exist only SV transmitted wave. The P transmitted wave becomes a surface wave.

(iii) For $s_T^- < s_0^1 < s_L^+ \Leftrightarrow \theta_0^2 < \theta_0 < \pi/2$: the P incident wave (6) creates no transmitted waves.

3.1.2. *The reflection and transmission coefficients*

Let $\bar{u}_n$ and $\bar{\sigma}_{n2}$ $(n = 1, 2)$ be the displacements and stresses of the reflected-transmitted waves traveling in the layer. Then, they are of the form (similar to the one of the incident wave)

$$\bar{u}_n = \bar{U}_n(y)\, e^{ik(x_1 - ct)}, \;\; \bar{\sigma}_{n2} = k\bar{T}_n(y)\, e^{ik(x_1-ct)}, \;\; n = 1, 2. \tag{26}$$

Let $\bar{\boldsymbol{\xi}}(y) = [\bar{U}_1(y) \;\; \bar{U}_2(y) \;\; \bar{T}_1(y) \;\; \bar{T}_2(y)]^T$. From the continuity conditions at $y = 0$ and $y = \varepsilon = kH$ we have

$$\bar{\boldsymbol{\xi}}(\varepsilon) = A_3\boldsymbol{\xi}_t^3 e^{i\varepsilon_3} + A_4\boldsymbol{\xi}_t^4 e^{i\varepsilon_4}, \;\; \bar{\boldsymbol{\xi}}(0) = \boldsymbol{\xi}_I^0 + A_1\boldsymbol{\xi}_r^1 + A_2\boldsymbol{\xi}_r^2, \tag{27}$$

where $\varepsilon_k = \varepsilon \cot\theta_k$ $(k = 3, 4)$ and $\boldsymbol{\xi}_I^0, \boldsymbol{\xi}_r^1, \boldsymbol{\xi}_r^2, \boldsymbol{\xi}_t^3$ and $\boldsymbol{\xi}_t^4$ are given by (16), (20), (21), (24) and (25), respectively. On the other hand, according to Vinh et al. [13]

$$\bar{\boldsymbol{\xi}}(0) = \mathbf{T}\bar{\boldsymbol{\xi}}(\varepsilon), \tag{28}$$

where the transfer matrix $\mathbf{T}$ is given by

$$\mathbf{T} = \begin{bmatrix} \dfrac{[\bar{\gamma};\cosh\varepsilon]}{[\bar{\gamma}]} & \dfrac{-i[\bar{\beta};\sinh\varepsilon]}{[\bar{\alpha};\bar{\beta}]} & \dfrac{-[\bar{\alpha};\sinh\varepsilon]}{[\bar{\alpha};\bar{\beta}]} & \dfrac{-i[\cosh\varepsilon]}{[\bar{\gamma}]} \\ \dfrac{-i[\bar{\gamma};\bar{\alpha}\sinh\varepsilon]}{[\bar{\gamma}]} & \dfrac{[\bar{\alpha}\cosh\varepsilon;\bar{\beta}]}{[\bar{\alpha};\bar{\beta}]} & \dfrac{-i\bar{\alpha}_1\bar{\alpha}_2[\cosh\varepsilon]}{[\bar{\alpha};\bar{\beta}]} & \dfrac{-[\bar{\alpha}\sinh\varepsilon]}{[\bar{\gamma}]} \\ \dfrac{-[\bar{\gamma};\bar{\beta}\sinh\varepsilon]}{[\bar{\gamma}]} & \dfrac{-i\bar{\beta}_1\bar{\beta}_2[\cosh\varepsilon]}{[\bar{\alpha};\bar{\beta}]} & \dfrac{[\bar{\alpha};\bar{\beta}\cosh\varepsilon]}{[\bar{\alpha};\bar{\beta}]} & \dfrac{i[\bar{\beta}\sinh\varepsilon]}{[\bar{\gamma}]} \\ \dfrac{-i\bar{\gamma}_1\bar{\gamma}_2[\cosh\varepsilon]}{[\bar{\gamma}]} & \dfrac{[\bar{\beta};\bar{\gamma}\sinh\varepsilon]}{[\bar{\alpha};\bar{\beta}]} & \dfrac{-i[\bar{\alpha};\bar{\gamma}\sinh\varepsilon]}{[\bar{\alpha};\bar{\beta}]} & \dfrac{[\bar{\gamma}\cosh\varepsilon]}{[\bar{\gamma}]} \end{bmatrix}, \tag{29}$$

here $\varepsilon_n = \varepsilon\bar{b}_n$, $n = 1, 2$ and

$$[f;g] = f_2g_1 - f_1g_2, \;\; [f] = f_2 - f_1, \tag{30}$$

$$\bar{\beta}_n = \bar{c}_{66}(\bar{b}_n - \alpha_n), \;\; \bar{\gamma}_n = \bar{c}_{12} + \bar{c}_{22}\bar{b}_n\bar{\alpha}_n, \;\; n = 1, 2, \tag{31}$$

$$\bar{\alpha}_n = -\frac{(\bar{c}_{12} + \bar{c}_{66})\bar{b}_n}{\bar{c}_{22}\bar{b}_n^2 - \bar{c}_{66} + \bar{X}}, \;\; n = 1, 2, \;\; \bar{X} = \bar{\rho}c^2, \tag{32}$$

$$\bar{b}_1 = \sqrt{\frac{\bar{S} + \sqrt{\bar{S}^2 - 4\bar{P}}}{2}}, \ \bar{b}_2 = \sqrt{\frac{\bar{S} - \sqrt{\bar{S}^2 - 4\bar{P}}}{2}}, \tag{33}$$

$$\bar{S} = \frac{\bar{c}_{22}(\bar{c}_{11} - \bar{X}) + \bar{c}_{66}(\bar{c}_{66} - \bar{X}) - (\bar{c}_{12} + \bar{c}_{66})^2}{\bar{c}_{22}\bar{c}_{66}}, \tag{34}$$

$$\bar{P} = \frac{(\bar{c}_{11} - \bar{X})(\bar{c}_{12} + \bar{c}_{66})^2}{\bar{c}_{22}\bar{c}_{66}}. \tag{35}$$

From (27) and (28) it follows

$$\boldsymbol{\xi}_I^0 + A_1\boldsymbol{\xi}_r^1 + A_2\boldsymbol{\xi}_r^2 = \mathbf{T}(A_3\boldsymbol{\xi}_t^3 e^{i\varepsilon_3} + A_4\boldsymbol{\xi}_t^4 e^{i\varepsilon_4}). \tag{36}$$

This equation can be rewritten as

$$\mathbf{PA} = \boldsymbol{\xi}_I^0, \tag{37}$$

where $\mathbf{A} = [A_1 \quad A_2 \quad A_3 \quad A_4]^T$ and

$$\mathbf{P} = -[\boldsymbol{\xi}_r^1 \quad \boldsymbol{\xi}_r^2 \quad \mathbf{0} \quad \mathbf{0}] + \mathbf{T}[\mathbf{0} \quad \mathbf{0} \quad \boldsymbol{\xi}_t^3 e^{i\varepsilon_3} \quad \boldsymbol{\xi}_t^4 e^{i\varepsilon_4}]. \tag{38}$$

The solution of Eq. (38) is

$$\mathbf{A} = \mathbf{P}^{-1}\boldsymbol{\xi}_I^0. \tag{39}$$

Eq. (39) is the closed-form expressions for the reflection and transmission coefficients.

3.2. Interfaces of general type

For interfaces of arbitrary type, such as tooth-saw-type interface and sin-type interface (Fig. 6), the results on reflected and transmitted waves presented in Subsection 3.1.1 are still valid. However, since the material layer $0 < x_2 < H$ now is *inhomogeneous*, according to (10), matrix $\mathbf{T}$ in formula (39) (being the transfer matrix of a *homogeneous* orthotropic elastic layer, given by (29)) must be replaced by the transfer matrix of *inhomogeneous* orthotropic elastic layer.

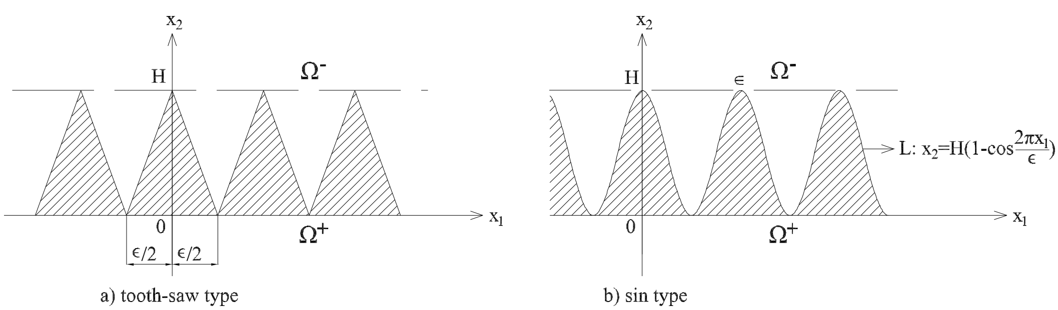

Fig. 6. Interfaces of tooth-saw type and sin type

To get this matrix, we divide the *inhomogeneous* layer $[0, H]$ into N *homogeneous* sub-layers with the same thickness $\delta = H/N$ by points $x_2^{(n)}$ $(n = 1, ..., N+1, x_2^{(1)} = 0, x_2^{(N+1)} = H)$. For n-th sub-layer occupying the domain $x_2^{(n)} < x_2 < x^{(n+1)}$ we take: $c_{ij} = c_{ij}(x_2^{(n)})$.

The contact between the sub-layers is welded. As n-th sub-layer is *homogeneous* and orthotropic, its transfer matrix, say $\mathbf{T}_n$, is given by (29). The transfer matrix $\mathbf{T}$ of the *inhomogeneous* layer $0 < x_2 < H$ is approximately computed by

$$\mathbf{T} = \mathbf{T}_1\,\mathbf{T}_2 ... \mathbf{T}_N. \tag{40}$$

It is not difficult to prove that the approximate transfer matrix $\mathbf{T}$ *tends to the exact transfer matrix of the inhomogeneous layer* $0 < x_2 < H$ *when* δ *tends to zero.*

Note that for the tooth-saw-type and sin-type interfaces, the average value of quantities is calculated by

$$\langle\phi\rangle = \frac{x_2}{H}\phi^+ + (1 - \frac{x_2}{H})\phi^-, \tag{41}$$

and

$$\langle\phi\rangle = \frac{1}{\pi}\arccos(1 - \frac{2x_2}{H})\phi^- + \big[1 - \frac{1}{\pi}\arccos(1 - \frac{2x_2}{H})\big]\phi^+. \tag{42}$$

4. NUMERICAL EXAMPLES

In this section, some numerical examples are carried out to examine the dependence of the reflection and transmission coefficients (RTCs), computed by Eq. (39), on the incident angle θ_0, the dimensionless frequency $e = k_0 H$ of the incident wave and the geometrical parameter $f = a/(a+b)$ of the tooth-comb interface. For computation, we take

$$\lambda^- = 7.59 \times 10^{10}\ \mathrm{Nm}^{-2}; \mu^- = 1.89 \times 10^{10}\ \mathrm{Nm}^{-2}; \rho^- = 2.19 \times 10^3\ \mathrm{kgm}^{-3}, \tag{43}$$

for the upper half-space Ω^- and

$$\lambda^+ = 9.4 \times 10^{10}\ \mathrm{Nm}^{-2}; \mu^+ = 4.0 \times 10^{10}\ \mathrm{Nm}^{-2}; \rho^+ = 1.74 \times 10^3\ \mathrm{kgm}^{-3}, \tag{44}$$

for the lower half-space Ω^+. The material parameters of the elastic layer are calculated by Eq. (9) along with Eq. (11), Eq. (41) or Eq. (42) depending on that the interface is of tooth-comb type, tooth-saw type or sin type, respectively.

From (43) and (44) it follows: $0 < s_L^+ < s_L^-$. According to the argument of Subsection 3.1.1 (b, c), there are two reflected waves and two transmitted waves for any $\theta_0 \in (0, \pi/2)$.

Fig. 7 shows the variation of the RTCs against the incident angle for the tooth-comb-type interface (Fig. 7(a)) (with $f = 0.3$), the tooth-saw-type interface (Fig. 7(b)) and the sin-type interface (Fig. 7(c)). It is seen from Fig. 7 that the variations of the RTCs corresponding to the tooth-saw-type and sin-type interfaces are similar. However, they are different from the one corresponding to the tooth-comb-type interface. The RTC-curves for the latter case are smooth than the ones for two former cases.

Fig. 8 represents the dependance of RTCs on the incident angle for a very rough interface of tooth-comb type (with $f = 0.3$) (solid lines) and for a plane interface ($f = 0$ or $f = 1$) (dashed lines). It is clear from Fig. 8 that the roughness of interfaces affects strongly the RTCs.

Fig. 9 shows the dependence the RTCs on the dimensionless incident wave frequency e for the tooth-comb-type interface (with $f = 0.3$) at $\theta_0 = \pi/4$. It is seen that

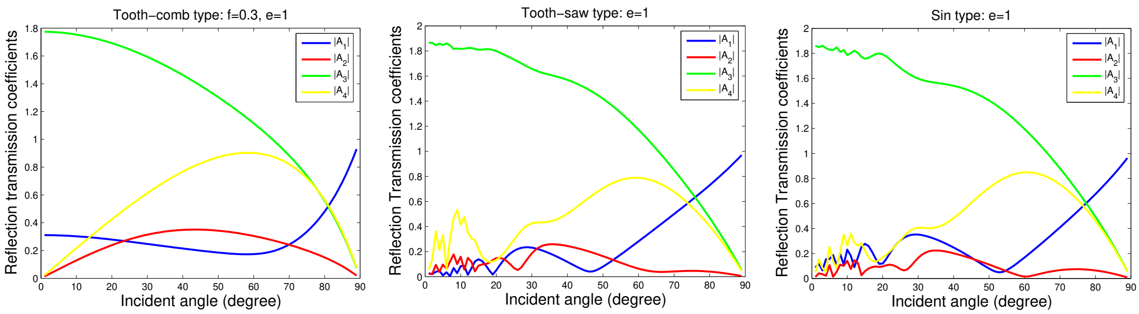

(a) (b) (c)

Fig. 7. Variation of RTCs against the incident angle for three types of interface

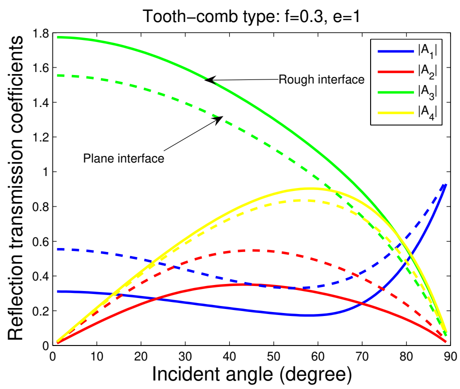

Fig. 8. Effect of the roughness of interfaces on the RTCs

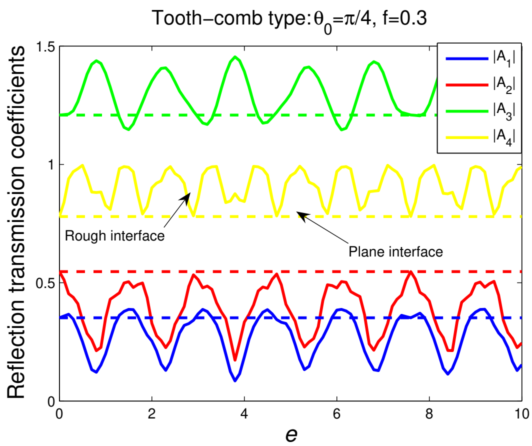

Fig. 9. Variation of the RTCs against the dimensionless incident wave frequency $e = k_0 H$

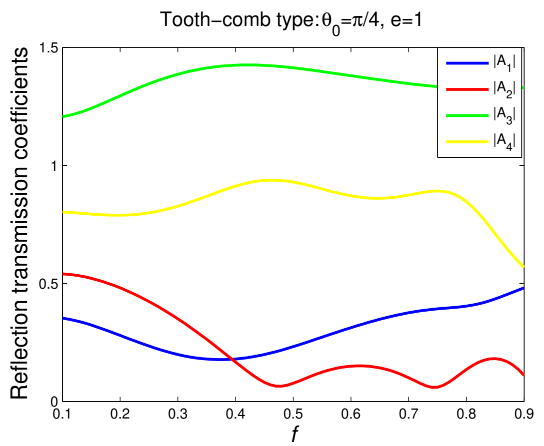

Fig. 10. Variation of the RTCs against the geometrical parameter f of a tooth-comb-type interface

the RTCs oscillate for the tooth-comb interface and become constant for the plane interface. This fact says again that the roughness of interfaces affects strongly the RTCs.

Fig. 10 presents the variation of the RTCs against the geometric parameter f of a very rough interface of tooth-comb type at $\theta_0 = \pi/4$ and $e = 1$. One can see that the geometric parameter f affects considerably on the RTCs.

It is noted that the numerical results given in Figs. 7–10 have been verified by means of the energy balance that needs to be satisfied, i.e. by means of the energy conversion carried out between the incident wave and the reflected and transmitted waves.

5. CONCLUSIONS

In this paper, the reflection and transmission of P-waves at a very rough interface between two isotropic elastic solids is investigated. Based on the obtained results on the homogenization of very rough interfaces between two isotropic elastic solids, the problem is considered as the reflection and transmission of P-waves through an inhomogeneous orthotropic elastic layer. Employing the transfer matrix of an orthotropic elastic layer, formulas in closed-form of the reflection and transmission coefficient have been derived. These formulas will be a good tool for determining the internal characteristics of the Earth crust from the signals of reflected and transmitted waves. Based on them, some numerical examples are carried out to examine the reflection and transmission of P-waves at a very rough interface of tooth-comb type, tooth-saw type and sin type. It is found from numerical results that the RTCs depend strongly on the incident angle, the incident wave frequency and:

(i) The type of rough interface affects strongly the variation of RTCs against the incident angle: the variation corresponding to the tooth-comb-type interface is smooth than that corresponding to the tooth-saw-type interface and the sin-type interface.

(ii) The roughness of interfaces makes the reflection coefficients decreasing and the transmission coefficient increasing. That means the roughness obstructs the reflection and support the transmission.

ACKNOWLEDGEMENT

The work was supported by the Vietnam National Foundation for Science and Technology Development (NAFOSTED) under grant number 107.02-2019.314.

REFERENCES

[1] D. C. Stickler. Scattering from a soft slightly rough surface. *Wave Motion*, **13**, (1991), pp. 211–221. https://doi.org/10.1016/0165-2125(91)90059-w.

[2] S. S. Singh and S. K. Tomar. qP-wave at a corrugated interface between two dissimilar pre-stressed elastic half-spaces. *Journal of Sound and Vibration*, **317**, (2008), pp. 687–708. https://doi.org/10.1016/j.jsv.2008.03.036.

[3] M. van Dyke. *Pertubation methods in fluid mechanics*. Parabolic, Stanford, CA, (1975).

[4] D. Talbot, J. Titchener, and J. Willis. The reflection of electromagnetic waves from very rough interfaces. *Wave Motion*, **12**, (1990), pp. 245–260. https://doi.org/10.1016/0165-2125(90)90042-3.

[5] P. C. Vinh, D. X. Tung, and N. T. Kieu. Homogenization of very rough two-dimensional interfaces separating two dissimilar poroelastic solids with time-harmonic motions. *Mathematics and Mechanics of Solids*, **24**, (2018), pp. 1349–1367. https://doi.org/10.1177/1081286518794227.

[6] A. Bensoussan, J. B. Lions, and J. Papanicolaou. *Asymptotic analysis for periodic structures*. North-Holland, Amsterdam, (1978).

[7] W. Kohler, G. Papanicolaou, and S. Varadhan. Boundary and interface problems in regions with very rough boundaries. In *Multiple Scattering and Waves in Random Media*, North-Hollands, Amsterdam, (1981).

[8] J. Nevard and J. B. Keller. Homogenization of rough boundaries and interfaces. *SIAM Journal on Applied Mathematics*, **57**, (1997), pp. 1660–1686. https://doi.org/10.1137/s0036139995291088.

[9] P. C. Vinh and D. X. Tung. Homogenized equations of the linear elasticity in two-dimensional domains with very rough interfaces. *Mechanics Research Communications*, **37**, (2010), pp. 285–288. https://doi.org/10.1016/j.mechrescom.2010.02.006.

[10] P. C. Vinh and D. X. Tung. Homogenization of very rough interfaces separating two piezoelectric solids. *Acta Mechanica*, **224**, (2013), pp. 1077–1088. https://doi.org/10.1007/s00707-012-0804-z.

[11] P. C. Vinh and D. X. Tung. Homogenization of rough two-dimensional interfaces separating two anisotropic solids. *Journal of Applied Mechanics*, **78**, (2011). https://doi.org/10.1115/1.4003722.

[12] J. D. Achenbach. *Wave propagation in elastic solids*. North-Holland, Amsterdam, (1973).

[13] P. C. Vinh, V. T. N. Anh, and N. T. K. Linh. On a technique for deriving the explicit secular equation of Rayleigh waves in an orthotropic half-space coated by an orthotropic layer. *Waves in Random and Complex Media*, **26**, (2016), pp. 176–188. https://doi.org/10.1080/17455030.2015.1132859.